Electronic Supplementary Material (ESI) for Dalton Transactions.

Supporting Information

One-Step Synthesis of Few-layer Nb_2CT_x MXene as Promising Anode Material for high-rate Lithium Ion Batteries

Jiabao Zhao, Jing Wen, Lina Bai, Junpeng Xiao, Rudong Zheng, Xinyuan Shan, lu li, Hong Gao *, Xitian Zhang

Key Laboratory for Photonic and Electronic Bandgap Materials, Ministry of Education, School of Physics and Electronic Engineering, Harbin Normal University, Harbin 150025, People's Republic of China

Experimentation

Synthesis of the accordion-like m-Nb_2CT_x : 0.5 g Nb_2AlC powder, −200 mesh, were immersed in 40% aqueous hydrofluoric solution, HF, for 70 h at 60 °C under continuous stirring. Afterwards, the mixture was washed by centrifugal machine at 9000 rpm, through several cycles of ultrapure water until the supernatant reached a pH of approximately 5. The speed was reduced to 5000 rpm, but no suspension was found after centrifugation. So the precipitate was collected by vacuum filtration. Put Nb_2CT_x precipitation in the vacuum drying oven, drying at 60 ℃ for 12 h.

Electrochemical testing : The electrochemical performance of the f-Nb_2CT_x and m-Nb_2CT_x electrode were tested in the 2016 coin type cell configurations. The working electrode was prepared by mixing active materials with acetylene black and polyvinylidene fluoride at a weight ratio of 80:10:10 on copper foils, and a Li foil was used as the counter electrode [1]. The electrolyte was 1 M $LiPF_6$ in a mixture of ethylene carbonate/dimethyl carbonate/ethylmethyl carbonate (EC/DEMC/EMC) solvent (volume ratio of EC/DMC/EMC = 1:1:1). Nickel foams were used as shims to help the current collectors contact with the cathode or the anode. The charge and discharge performance were conducted with a LAND-CT2001A test system at the room temperature. The cyclic voltammetry (CV) and the galvanostatic discharge/charge (GDC) were performed on an electrochemical workstation (Bio-logic VMP-3, France) under a potential window of 0.01-3.0 V.

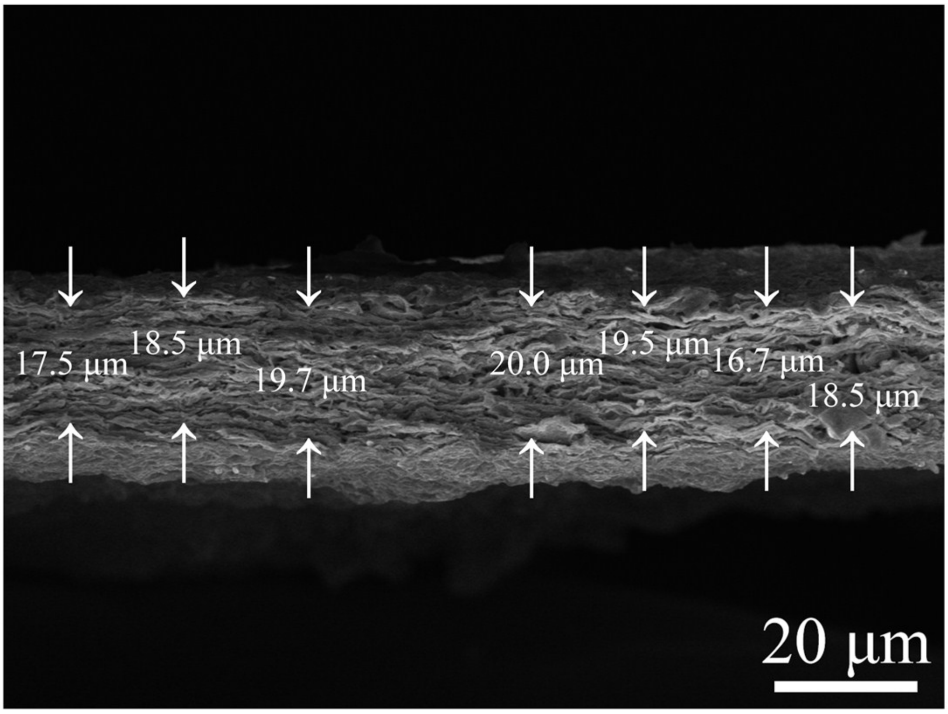

Fig. S1 Measured thicknesses at different positions of the Nb_2CT_x film. The average thickness of the paper is calculated to be approximately 18.6 μm.

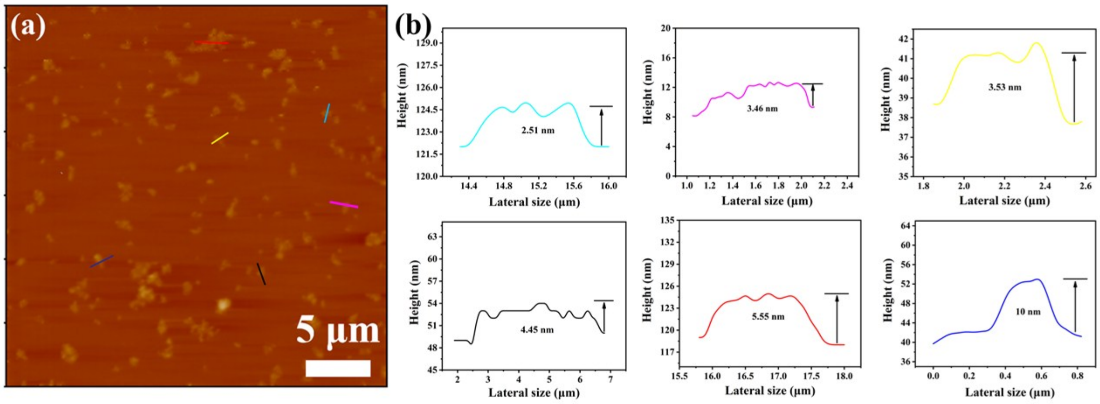

Fig. S2 (a) AFM image of the f-Nb_2CT_x. (b) thicknesses of f-Nb_2CT_x nanosheets.

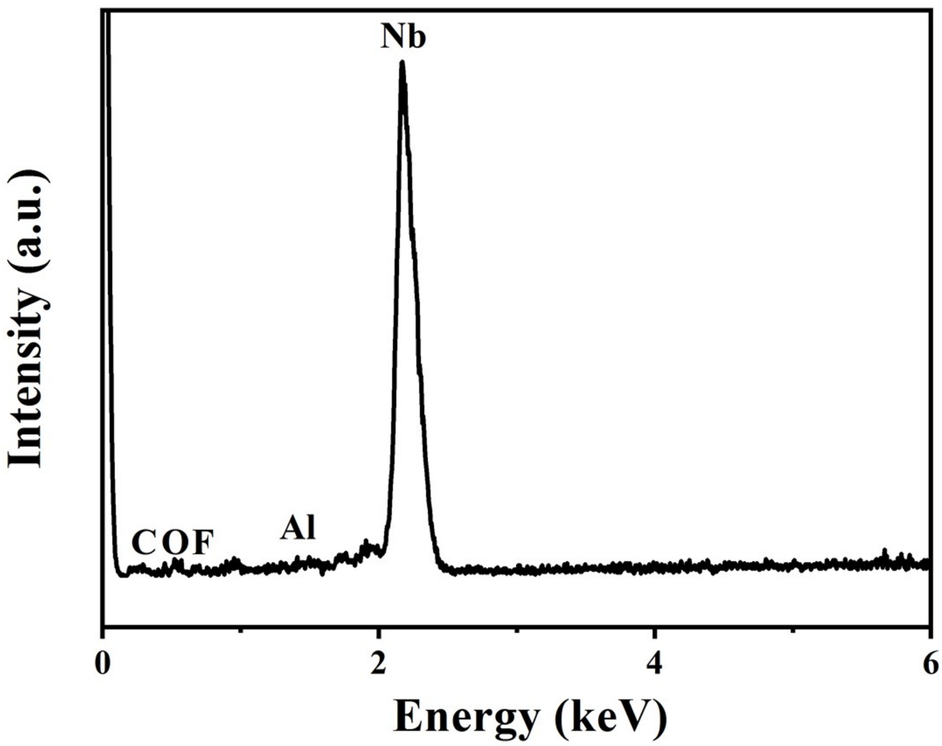

Fig. S3 EDX spectrum of the Nb_2CT_x film is mainly composed of Nb, C, O, F and a small amount of Al elements.

Table S1. Composition content of Nb_2CT_x films. The Nb : C : O : F : Al atomic ratio determined by EDS were found to be 53.11 : 27.48 : 15.35 : 3.33 : 0.73.

Element	Weigh%	Atomic%
Nb (K)	88.22	53.11
C (K)	5.90	27.48
O (K)	4.39	15.35
F (K)	1.13	3.33
Al (K)	0.35	0.73

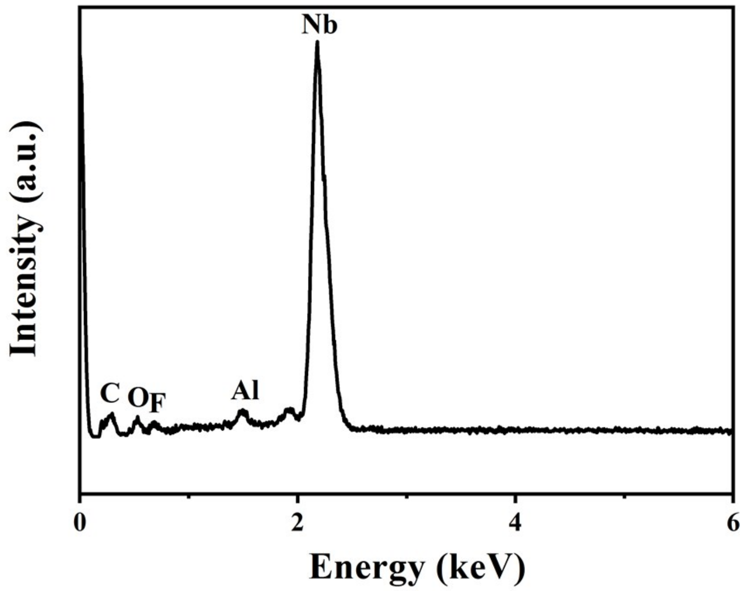

Fig. S4 The Nb : C : O : F : Al atomic ratio determined by EDS were found to be 52.31 : 27.84 : 10.60 : 8.44 : 0.82 (m-Nb_2CT_x).

Table S2. XPS peak fitting results for Nb_2C

Region	BE (eV)	Assigned to	Substance	Reference
C 1s	282.4	C-Nb	Nb_2C	2
	284.8	C-C	C	3
	286.4	C-O	$Nb_2C\text{-}O_x$	4
	288.6	C=O		5
O 1s	530.3	Nb-O	Nb_2O_5	2
	530.9	-O	$Nb_2C\text{-}O_x$	6
	532.2	O-H	$Nb_2C\text{-}(OH)_x$	7, 8
	533.5	O-C=O	C	7, 8
F 1s	684.6	-F	$Nb_2C\text{-}F_x$	9

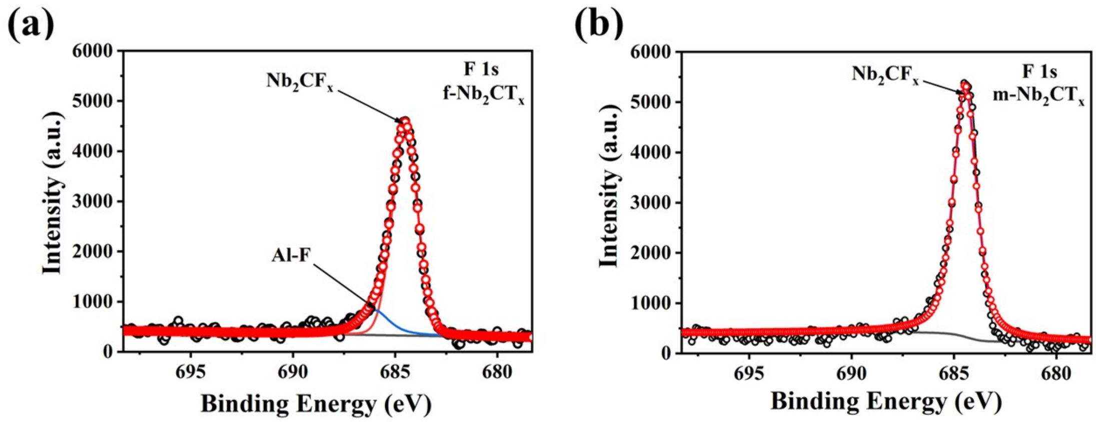

Fig. S5 F 1s spectra of (a) f-Nb_2CT_x and (b) m-Nb_2CT_x

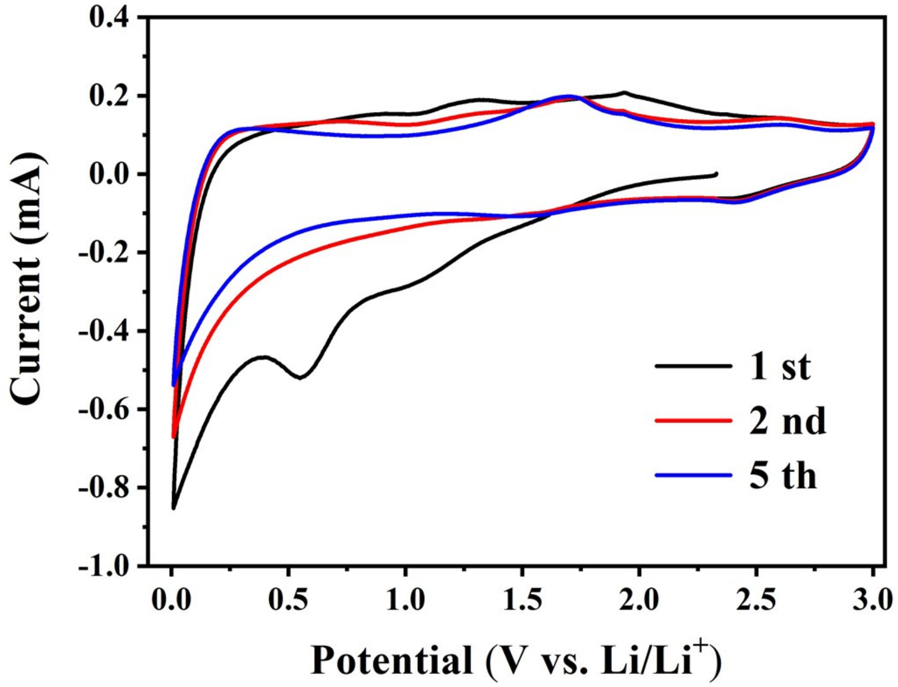

Fig. S6 CV curves of the m-Nb_2CT_x electrode at a scanning rate of 0.5 mV s^{-1}.

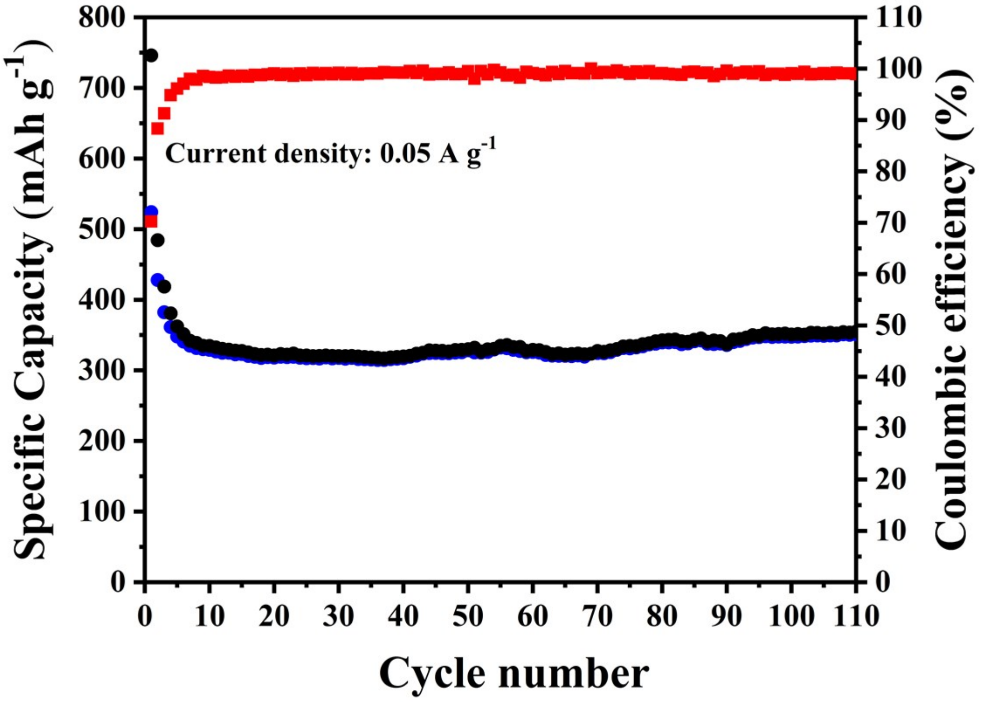

Fig. S7 Cycling performance of the f-Nb_2CT_x electrode at 0.05 A g^{-1}.

The exposed surface area of the m-Nb_2CT_x and f-Nb_2CT_x were further investigated by N2 sorption/desorption measurements. Fig. S8 shows the adsorption−desorption isotherm curve of m-Nb_2CT_x and f-Nb_2CT_x. The specific surface area of m-Nb_2CT_x is 14 m^2/g by the BET method. However, the f-Nb_2CT_x possesses a bigger specific surface area of 38 m^2/g, which is about 2.7 times larger than that of m-Nb_2CT_x. The high specific surface area is in favor of the exposure of active sites.

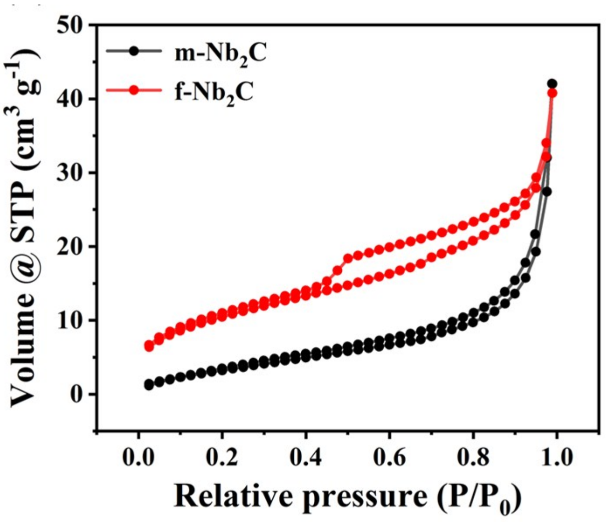

Fig. S8 N2 adsorption-desorption isotherms.

References

[1] S.P. Wu, R.Y. Ge, M.J. Lu, R. Xu, Z. Zhang, Nano Energy, 2015, 15, 379−405.

[2] W.L. Zhang, J.M. Tian, H.B. Zeng, J.Q. Liu, Y. Tian, Chemical Engineering Journal, 2019, 366, 321−329.

[3] L. Li, M.Y. Zhang, X.T. Zhang, Z.G. Zhang, Journal of Power Sources, 2017, 36, 4234−241.

[4] D.X. Yang, A. Velamakanni, G. Bozoklu, S. Park, M. Stoller, R.D. Piner, R.S. Ruoff, Carbon, 2009, 47, 145−152.

[5] Y.L. He, J.H. Li, K. Luo, L.F. Li, J.B. Chen, J.Y. Li, Ind. Eng. Chem. Res., 2016, 55, 3775-3781.

[6] J. Halim, S. Kota, M.R. Lukatskaya, Y. Gogotsi, Advanced Functional Materials, 2016, 26, 3118−3127.

[7] H.R. Byon, B.M. Gallant, S. Woo, Y. Shao-Horn, Advanced Functional Materials, 2013, 23, 1037-1045.

[8] S.H. Kundu, Y.M. Wang, W.Xia, M. Muhler, J. Phys. Chem., 2008, 112, 16869-16878.

[9] Y.D. Agnese, M.R. Lukatskaya, K.M. Cook, P.L. Taberna, Y. Gogotsi, P. Simon, Electrochem. Commun., 2014, 48, 118-122.